

Lung Stem Cell Differentiation in Mice Directed by Endothelial Cells via a BMP4-NFATc1-Thrombospondin-1 Axis

Joo-Hyeon Lee,^{1,2,3} Dong Ha Bhang,⁴ Alexander Beede,^{1,2,3} Tian Lian Huang,^{5,6} Barry R. Stripp,⁷ Kenneth D. Bloch,⁸ Amy J. Wagers,^{9,10,11} Yu-Hua Tseng,^{5,6} Sandra Ryeom,⁴ and Carla F. Kim^{1,2,3,*}

¹Stem Cell Program, Boston Children's Hospital, Boston, MA 02115, USA

²Harvard Stem Cell Institute, Cambridge, MA 02138, USA

³Department of Genetics, Harvard Medical School, Boston, MA 02115, USA

⁴Department of Cancer Biology, Abramson Family Cancer Research Institute, University of Pennsylvania School of Medicine, Philadelphia, PA 19104, USA

⁵Section on Integrative Physiology and Metabolism, Joslin Diabetes Center, Harvard Medical School, Boston, MA 02215, USA

⁶Harvard Stem Cell Institute, Harvard University, Cambridge, MA 02138, USA

⁷Women's Guild Lung Institute, Department of Medicine, Cedars-Sinai Medical Center, Los Angeles, CA 90048, USA

⁸Anesthesia Center for Critical Care Research and Cardiovascular Research Center, Massachusetts General Hospital, Boston, MA 02114, USA

⁹Harvard Stem Cell Institute, Department of Stem Cell and Regenerative Biology, Harvard University, Cambridge, MA 02138, USA

¹⁰Joslin Diabetes Center, Boston, MA 02215, USA

¹¹Howard Hughes Medical Institute, Chevy Chase, MD 20815, USA

*Correspondence: carla.kim@childrens.harvard.edu

<http://dx.doi.org/10.1016/j.cell.2013.12.039>

SUMMARY

Lung stem cells are instructed to produce lineage-specific progeny through unknown factors in their microenvironment. We used clonal 3D cocultures of endothelial cells and distal lung stem cells, bronchioalveolar stem cells (BASCs), to probe the instructive mechanisms. Single BASCs had bronchiolar and alveolar differentiation potential in lung endothelial cell cocultures. Gain- and loss-of-function experiments showed that BMP4-Bmpr1a signaling triggers calcineurin/NFATc1-dependent expression of thrombospondin-1 (*Tsp1*) in lung endothelial cells to drive alveolar lineage-specific BASC differentiation. *Tsp1* null mice exhibited defective alveolar injury repair, confirming a crucial role for the BMP4-NFATc1-TSP1 axis in lung epithelial differentiation and regeneration in vivo. Discovery of this pathway points to methods to direct the derivation of specific lung epithelial lineages from multipotent cells. These findings elucidate a pathway that may be a critical target in lung diseases and provide tools to understand the mechanisms of respiratory diseases at the single-cell level.

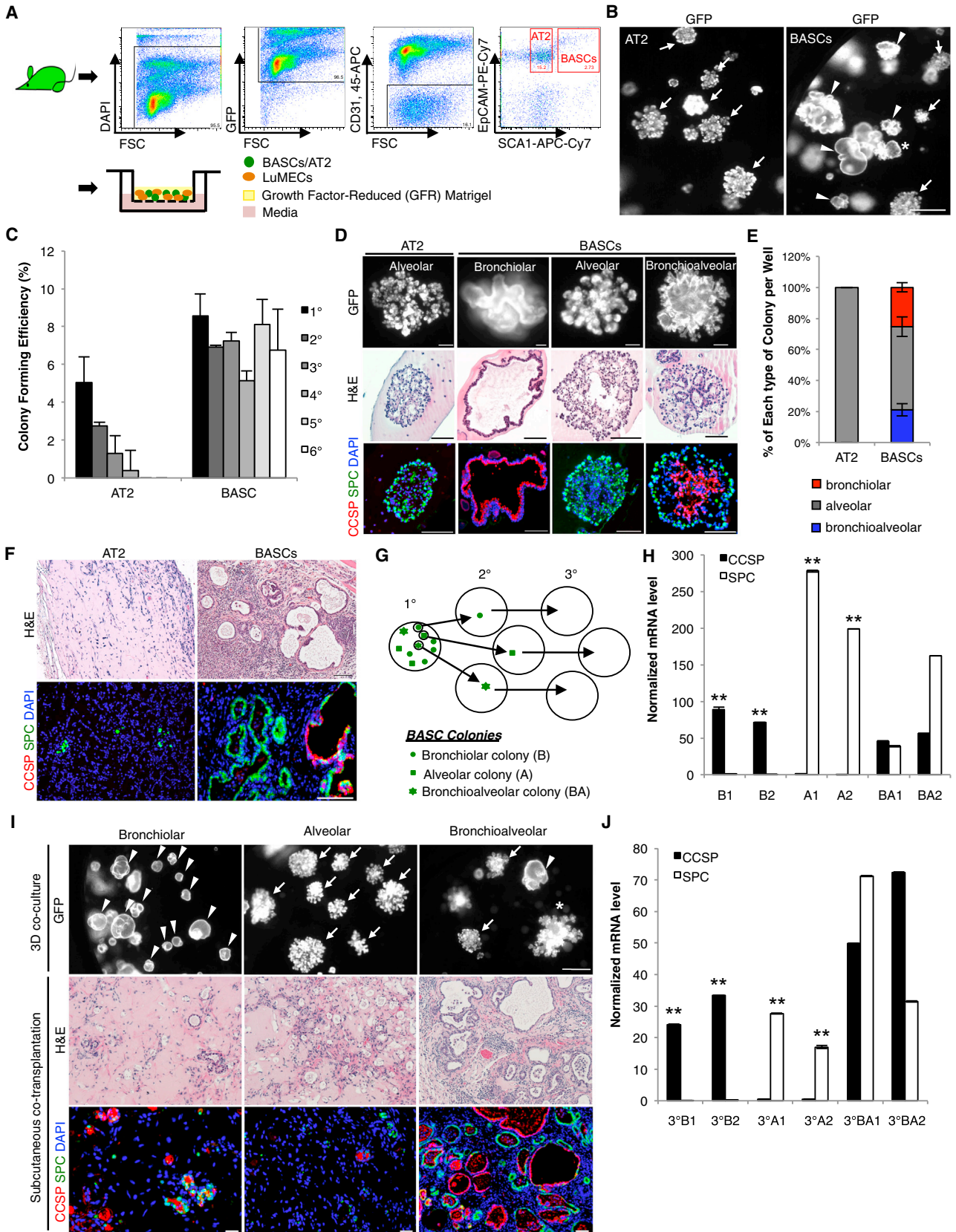
INTRODUCTION

Adult tissue stem cells reside in specialized niches containing supporting cells and factors that control stem cell survival, self-renewal, and differentiation (Jones and Wagers, 2008; Morrison and Spradling, 2008).

Lung epithelial repair is governed by stem/progenitor cell populations in distinct niches along the proximal-distal axis (e.g., Rawlins et al., 2009; Rock et al., 2011; Otto, 2002). Crosstalk between lung stem/progenitor cells and their niche is likely pivotal for maintaining the balance of stem and differentiated cells. Defects in such interactions may lead to acute respiratory distress syndrome, bronchopulmonary dysplasia, chronic obstructive pulmonary disease, idiopathic pulmonary fibrosis, and cancer. However, little is known about the supporting cells affecting lung regenerative potential or the precise mechanisms regulating differentiation and repair.

Bronchioalveolar stem cells (BASCs) are adult murine distal lung epithelial stem cells that reside in the bronchioalveolar duct junction, where the airways open to the alveolar space. BASCs coexpress the bronchiolar club cell (Clara) marker, CCSP (club cell [Clara] secretory protein [Scgb1a]), and the alveolar type 2 cell (AT2) marker, SPC (prosurfactant protein C) (Kim et al., 2005). Fluorescence-activated cell sorting (FACS)-enriched BASCs self-renew and differentiate in 2D culture systems and proliferate in response to bronchiolar and alveolar lung injury (Dovey et al., 2008; Kim et al., 2005; Zacharek et al., 2011). Lineage-tracing studies showed that BASCs can give rise to alveolar epithelial cells in vivo (Rock et al., 2011; Tropea et al., 2012). Multiple stem/progenitor cell populations in the adult distal lung, including BASCs, club cells, AT2 cells, and integrin- α -6-expressing alveolar progenitors, may contribute to homeostasis and repair (Barkauskas et al., 2013; Chapman et al., 2011; Rawlins et al., 2009; Rock et al., 2011; Tropea et al., 2012). Clonal analysis of these cells has not been feasible, limiting understanding of lung stem cells.

3D Matrigel-based culture systems mimicking the niche have advanced the lung stem cell field. Distal lung epithelial



(legend on next page)

stem/progenitor cells required support cells such as fibroblasts to form epithelial colonies (Kim et al., 2005; Lee et al., 2013; McQualter et al., 2010; Teisanu et al., 2011). The distal lung is highly vascularized, and numerous studies show an important role for the vasculature in lung development (DeLisser et al., 2006; Jakkula et al., 2000). Endothelial-derived Mmp14 is crucial for AT2 cell proliferation during lung regeneration (Ding et al., 2011). Although these studies have laid an important framework, it is not known how lineage-specific differentiation of lung stem cells is regulated by stroma. Here, we identify a bone morphogenetic protein 4 (BMP4)-nuclear factor of activated T cell c1 (NFATc1)-thrombospondin-1 (TSP1) signaling axis in endothelial cells that is critical for alveolar specification of BASC differentiation.

RESULTS

Lung Endothelial Cells Support Stem Cell Properties of BASCs

Given the intimate spatial relationship between lung epithelium and endothelial cells, we asked whether endothelial cells support 3D epithelial growth. CD31⁺CD45⁻EpCAM⁺Sca1⁻ cells (enriched for AT2 cells, AT2 hereafter) or CD31⁻CD45⁻EpCAM⁺Sca1⁺ cells (enriched for putative BASCs, BASCs hereafter) from β -actin-GFP mice were cocultured with primary mouse lung endothelial cells (LuMECs) (Figure 1A; Figures S1A and S1B available online). After 14 days, epithelial colonies were observed in AT2 cell and BASC cocultures (Figure 1B). Limiting

dilution assays showed that LuMECs supported BASC self-renewal (Figure S1C); BASCs were passaged multiple times in the presence of LuMECs without decreased colony-forming efficiency, whereas AT2 cell colony formation decreased with passage (Figures 1C and S1C).

Importantly, LuMECs supported BASC differentiation into multiple epithelial lineages. Three colony types arose in BASC/LuMEC cocultures: bronchiolar-like structures (bronchiolar colonies hereafter) with cells positive for CCSP; alveolar-like structures (alveolar colonies hereafter) expressing SPC; and mixed morphology structures (bronchioalveolar colonies hereafter, see below) containing CCSP-positive and SPC-positive cells (Figures 1B, 1D, and 1E). In contrast, AT2 cells only formed alveolar structures expressing SPC (Figures 1B, 1D, and 1E). Quantitative real-time PCR analysis confirmed the expression of CCSP and SPC in BASC colonies, yet no detectable expression of CCSP in AT2 cell colonies (Figure S1D). The alveolar type 1 (AT1) cell marker, T1 α , and the ciliated cell marker, FoxJ1, were detected in BASC cultures, whereas AT2 cultures only expressed SPC and T1 α (Figure S1E). Bronchiolar colonies also contained ciliated cells positive for acetylated-tubulin and goblet cells expressing MUC5AC (Figure S1F), but there was no expression of these markers in alveolar colonies (Figure S1G; data not shown). Mixed colonies contained cells positive for CCSP, acetylated-tubulin, MUC5AC, or SPC, and CCSP- and SPC-dual-positive cells (Figure S1H). We have termed mixed colonies "bronchioalveolar colonies." LuMECs also supported BASC differentiation after subcutaneous cotransplantation. BASCs, but

Figure 1. LuMECs Support BASC Self-Renewal and Differentiation In Vitro and In Vivo

(A) Schematic of FACS strategy to enrich for AT2 cells and BASCs from β -actin-GFP mice and 3D coculture with LuMECs. CD45-positive hematopoietic and CD31-positive endothelial cells were excluded. EpCAM-positive epithelial cells were selected. From these selections, Sca1-positive cells were BASCs, and Sca1-negative cells were AT2 cells.

(B) Representative images of GFP colonies from 3D coculture of AT2 cells (left) or BASCs (right) with LuMECs after 14 days. Arrowhead points to bronchiolar colony, arrow points to alveolar colony, and asterisk indicates bronchioalveolar colony. Scale bar, 500 μ m.

(C) Self-renewal of AT2 cells and BASCs in 3D LuMEC cocultures. Primary colonies (1^o) were dissociated, and GFP+ cells were replated for secondary (2^o) and subsequent (3^o, 4^o, 5^o, 6^o) colony formation. Colony forming efficiency is the number of colonies formed/number of cells plated per well as a percentage. Data presented are the mean of three independent experiments with triplicate wells. Error bars indicate SD.

(D) Representative GFP images of alveolar colonies from AT2 cells (top, left), and bronchiolar, alveolar, and bronchioalveolar colonies from BASCs (top, right). Hematoxylin and eosin staining (H&E; middle) and IF (bottom) for CCSP (red), SPC (green), and DAPI (blue) show BASC differentiation into club (Clara) cells and AT2 cells. Scale bars, 100 μ m.

(E) Quantification of each colony type from AT2 cell (n = 687) or BASC cocultures (n = 842). Of colonies, 25.4% were bronchiolar, 53.5% were alveolar, and 21.1% were mixed. The mean percentage of total colonies per well represented by each type of colony is shown. n, number of colonies scored. Data presented are the mean of seven independent experiments with triplicate wells. Error bars indicate SD.

(F) Subcutaneous cotransplantation of AT2 cells or BASCs mixed with LuMEC/Matrigel. H&E (top) and IF (bottom) for CCSP (red), SPC (green), and DAPI (blue) show that only BASCs coinjected with LuMECs formed epithelial structures with cells positive for CCSP, SPC, or both; BASCs, n = 7/8 mice injected formed epithelial structures; AT2 cells, n = 9/9 mice injected did not yield epithelial structures. Images are representative of three independent experiments. Scale bar, 100 μ m.

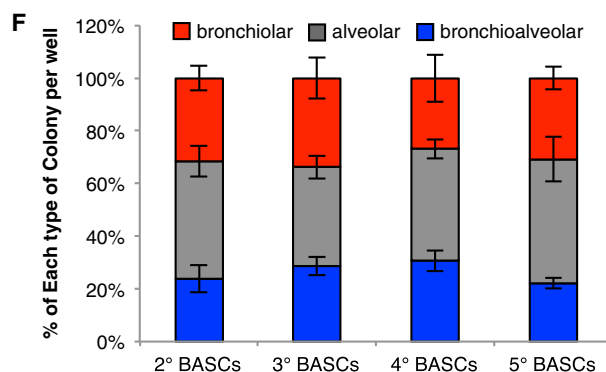
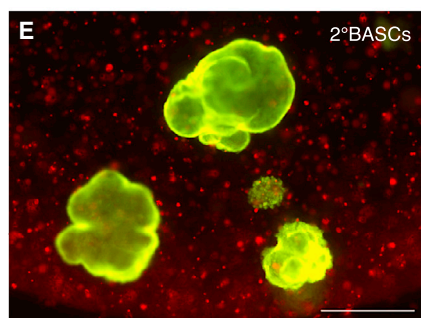
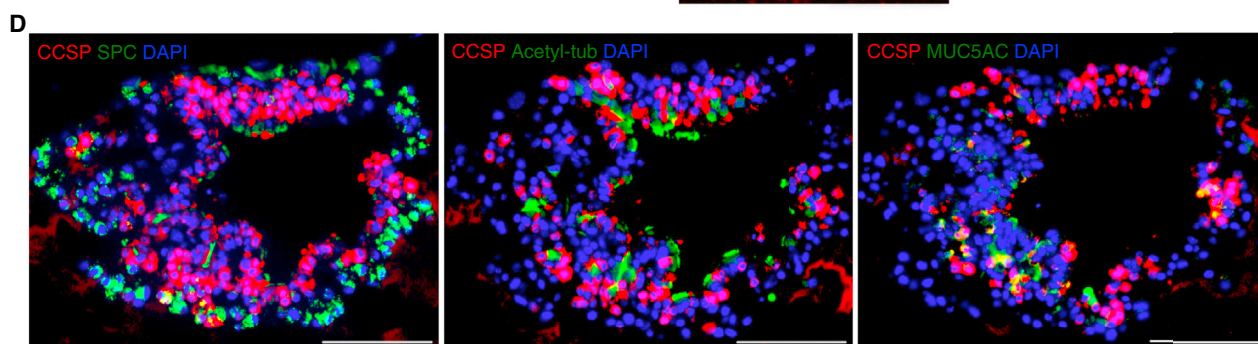
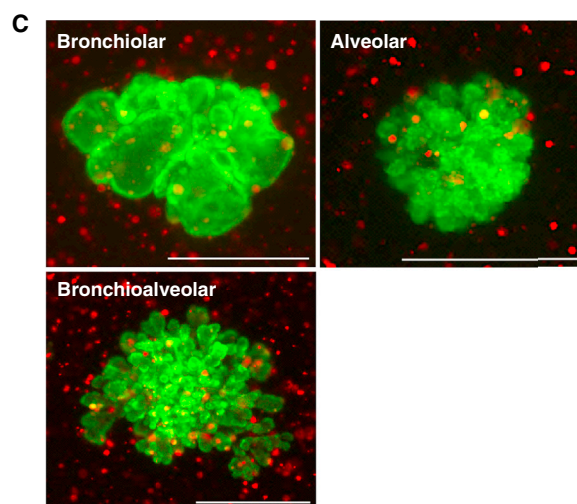
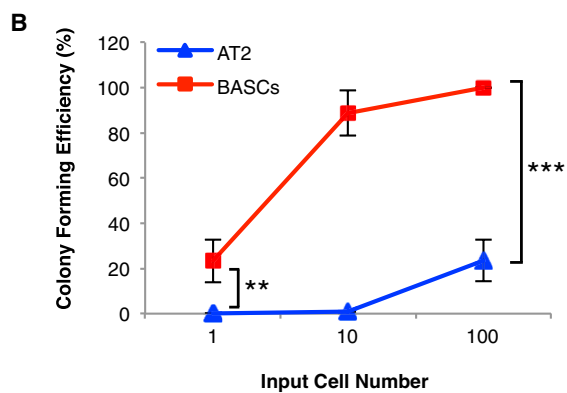
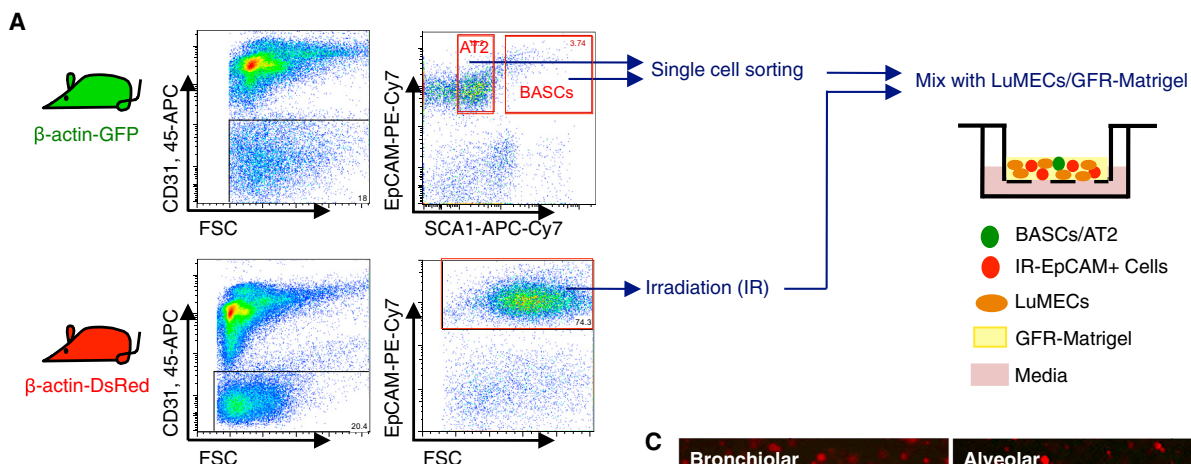
(G) Schematic of clonal serial passage analysis. The 1^o colonies were plated for 2^o or 3^o colony formation (I), and half of the cells were used for quantitative real-time PCR (H and J). Data shown are from 20 individual colonies per type analyzed over four independent experiments.

(H) Representative quantitative real-time PCR analysis validating expression of SPC (white bars) and CCSP (black bars) in cells from two different individual colonies. B1 and B2, primary bronchiolar colony; A1 and A2, primary alveolar colony; BA1 and BA2, primary bronchioalveolar colony. All are normalized to *Gapdh*. Data presented are the mean of triplicate wells. Error bars indicate SD (**p < 0.001).

(I) Representative GFP images of 2^o colonies from passage of each colony type. Arrowhead points to bronchiolar colony, arrow points to alveolar colony, and asterisk indicates bronchioalveolar colony. Scale bars, 500 μ m (top); H&E (middle) and IF (bottom) analysis for CCSP (red), SPC (green), and DAPI (blue) in tissue sections from subcutaneous transplantation of cells from BASC-derived bronchiolar (left) (n = 3/8 mice formed epithelial structures), alveolar (middle) (n = 15/15 mice did not yield epithelial structures), or bronchioalveolar colonies (right) (n = 9/9 mice generated epithelial structures). Scale bar, 100 μ m.

(J) Representative quantitative real-time PCR analysis in tertiary colonies as in (H). 3^oB1 and 3^oB2, tertiary bronchiolar colony; 3^oA1 and 3^oA2, tertiary alveolar colony; 3^oBA1 and 3^oBA2, tertiary bronchioalveolar colony. All are normalized to *Gapdh*. Data presented are the mean of triplicate wells. Error bars indicate SD (**p < 0.001).

See also Figure S1.



(legend on next page)

not AT2 cells, coinjected with LuMECs formed tube-like structures lined by epithelial cells expressing CCSP, SPC, or both (Figure 1F). These data suggested that LuMECs support BASC self-renewal and differentiation into bronchiolar and alveolar lineages in vitro and in vivo.

The derivation of multiple lineages in 3D cocultures could be a result of multipotent stem cell differentiation or the outgrowth of a mixture of cell types. BASCs from GFP or dsRed mice were mixed and cocultured with LuMECs. Colonies that arose were green or red, suggesting their clonal nature (Figure S1I). To further test multipotency, individual colonies were tested for secondary colony formation and differentiation (Figure 1G). Bronchioalveolar colonies gave rise to all three colony types with repeated passage, whereas bronchiolar colonies generated only bronchiolar colonies, and alveolar colonies only formed alveolar colonies (Figures 1H–1J, S1K, and S1L). Bronchioalveolar colonies retained efficient colony formation compared to bronchiolar colonies, and alveolar colonies had limited passaging capacity (Figures S1J and S1M). Bronchioalveolar colonies from BASC/LuMEC cocultures also exhibited multipotent differentiation capacity in vivo because they produced numerous lung epithelial structures consisting of acetylated-tubulin-, MUC5AC-, CCSP-, SPC-, or dual-positive CCSP/SPC cells after subcutaneous cotransplantation (Figures 1I, S1N, and S1O). Bronchiolar colonies generated rare epithelial structures, whereas alveolar colonies were unable to form epithelial structures (Figure 1I).

The ability of single cells to give rise to multiple lineages is a stem cell hallmark that has not been demonstrated in lung 3D cocultures. Single BASCs from GFP mice were cocultured with LuMECs and dsRed-labeled “helper cells” (irradiated EpCAM-positive lung epithelial cells) (Figure 2A). Single BASCs developed colonies of all three types, with bronchioalveolar colonies the predominant type (80%) (Figures 2B and 2C). Immunofluorescence (IF) confirmed the multilineage differentiation of these bronchioalveolar colonies (Figure 2D) with the continued ability to differentiate after multiple passages (Figures 2E and 2F).

Endothelial Cells Govern BASC Differentiation in an Organ-Specific Manner

Organ-specific endothelium has been implicated in other stem cell niches, so we isolated primary liver endothelial cells (LiMECs) (Figure S2) and cocultured them with BASCs. BASC/LiMEC cocultures had enhanced bronchiolar colony formation and reduced alveolar colony formation compared to BASC/

LuMEC cocultures (Figures 3A–3C). Passaged bronchioalveolar colonies also exhibited markedly expanded bronchiolar colony differentiation at the expense of alveolar colonies when cocultured with LiMECs (Figure 3D). Bronchioalveolar colonies arising from BASC/LuMEC cocultures were subcutaneously injected with LuMECs or LiMECs. LiMEC coinjections yielded primarily bronchiolar structures in contrast to the three different types of lung epithelial structures formed in LuMEC coinjections (Figures 3E and 3F), suggesting a specific requirement for lung endothelium in BASC differentiation.

TSP1 in Endothelial Cells Regulates BASC Differentiation

The necessity of lung endothelial cells in BASC differentiation suggested that endothelial factors are important for this process. TSP1, an angiogenesis inhibitor, is highly expressed in lung endothelial cells (Adams and Lawler, 2004; Chen et al., 2000; Lawler, 2002) and is upregulated developmentally when alveolar epithelial cells proliferate and differentiate (Iruela-Arispe et al., 1993; O’Shea and Dixit, 1988). Because TSP1 expression was significantly higher in LuMECs versus LiMECs (Figure 3G), we examined its role in BASC differentiation.

Lung injury models can identify proteins necessary for lung regeneration and differentiation. LuMECs were isolated at various times after naphthalene or bleomycin treatment, in vivo models of bronchiolar and alveolar epithelial injury, respectively, to examine *Tsp1* expression. *Tsp1* mRNA was significantly reduced in LuMECs 3 days after naphthalene treatment when regeneration of club cells occurs and restored 14 days after injury when regeneration is largely completed (Figure 4A). In contrast, bleomycin treatment led to higher *Tsp1* expression in LuMECs 14 days after injury when alveolar epithelial repair is underway (Figure 4A).

To gain insight into the necessity of TSP1 as a regulator of BASC differentiation, we tested *Tsp1*-deficient LuMECs in 3D cocultures. LuMECs were isolated from *Tsp1*^{-/-} mice (Lawler et al., 1998). *Tsp1*^{-/-} LuMECs modestly increased colony number in cocultures (Figure S3A). Strikingly, BASC/*Tsp1*^{-/-} LuMEC cocultures produced 3.2-fold more bronchiolar colonies and 3.5-fold fewer alveolar colonies than BASC/*Tsp1*^{+/+} LuMEC cocultures (Figures 4B and 4C). CCSP and SPC mRNA levels validated the enhanced bronchiolar differentiation phenotype with *Tsp1*^{-/-} LuMECs (Figure 4D). Altered differentiation was not due to a lineage-specific proliferation defect because bronchiolar or alveolar colonies cocultured with *Tsp1*^{-/-} LuMECs

Figure 2. Single BASCs Develop Multilineage Lung Organoids

(A) Schematic of “helper cell” 3D cocultures. Single GFP+ BASCs were mixed with irradiated EpCAM-positive dsRed lung epithelial cells and cocultured with LuMECs.

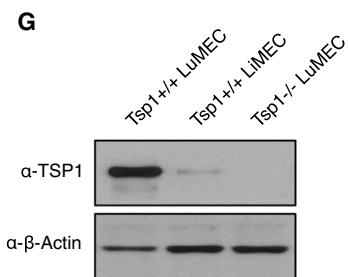
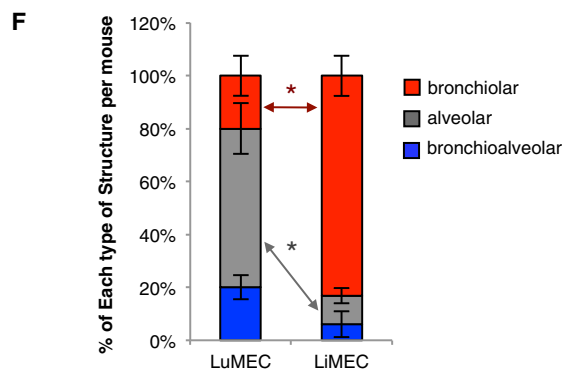
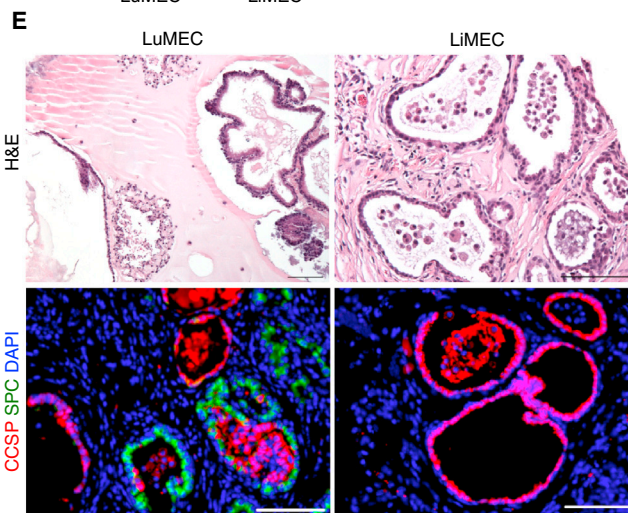
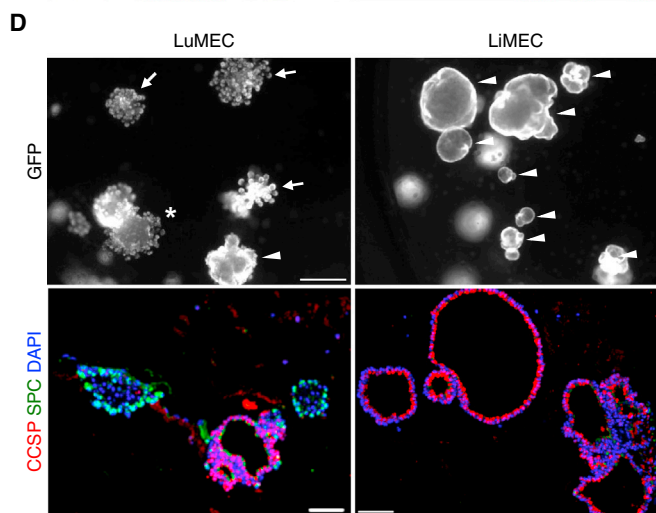
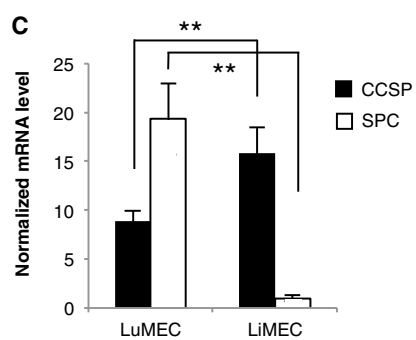
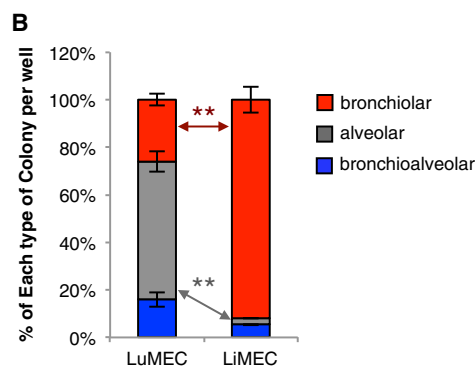
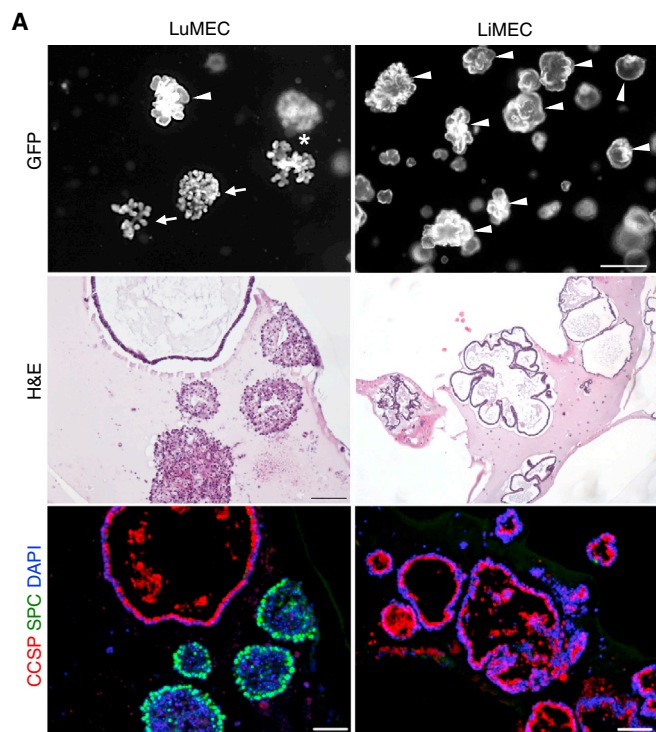
(B) Limiting dilution assay in helper cell 3D cocultures. The percentage of wells with colony formation from 1, 10, or 100 GFP+ cells for each population (BASCs in red; AT2 in blue) is shown. n = 180, 105, and 90 wells with 1, 10, or 100 cells plated, respectively. Data presented are the mean of four independent experiments with triplicate wells. Error bars indicate SD (**p < 0.001; ***p < 0.0001).

(C) Representative merged fluorescent images (GFP, dsRed) from single GFP+ BASC helper cell cocultures. Scale bars, 500 μm.

(D) Representative IF in a bronchioalveolar colony derived from a single BASC with CCSP (red), SPC (green), and DAPI (blue) (top), with CCSP (red), acetylated-tubulin (green), and DAPI (blue) (middle), and with CCSP (red), MUC5AC (green), and DAPI (blue) (bottom). Scale bars, 100 μm.

(E) Representative merged image (GFP, dsRed) of single BASC-derived secondary colonies. Scale bar, 500 μm.

(F) Quantification of colony types from single BASC-derived bronchioalveolar colonies (n = 14 bronchioalveolar colonies tested, n = 384 secondary colonies [2⁺ BASCs] scored) or from subsequent serial passage (n = 475 3⁺ BASCs, n = 465 4⁺ BASCs, n = 452 5⁺ BASCs). n, number of colonies scored. Data presented are the mean of three independent experiments with four individual colonies. Error bars indicate SD.



(legend on next page)

actually showed increased colony numbers (Figure S3B) and generated bronchiolar or alveolar colonies, respectively, as expected (Figure 4E). *Tsp1*^{-/-} BASCs exhibited differentiation capacity comparable to *Tsp1*^{+/+} BASCs (Figure S3I). Normal bronchiolar and alveolar differentiation was seen when equal numbers of *Tsp1*^{+/+} and *Tsp1*^{-/-} LuMECs were mixed for coculture with BASCs (Figures S3C–S3E). Finally, subcutaneous cotransplantation of bronchioalveolar colonies with *Tsp1*^{-/-} LuMECs yielded a significantly higher proportion of bronchiolar epithelial structures at the expense of alveolar structures compared with *Tsp1*^{+/+} LuMEC coinjections (Figures 4F–4H). Together, these data strongly suggested that TSP1 functions as a positive regulator of alveolar differentiation of BASCs in vitro and in vivo.

It was unclear whether TSP1 played a direct role or if a downstream factor affected BASC differentiation. TSP1 constitutes a major portion (~20%) of total platelet α granule content during platelet activation (Baenziger et al., 1971; Ganguly, 1971; Lawler et al., 1978). The addition of *Tsp1*^{+/+} platelet releasate (*Tsp1*^{+/+} PR) to BASC/*Tsp1*^{-/-} LuMEC cocultures increased alveolar colony formation and reduced bronchiolar colonies compared to controls (Figures S3F–S3H). Purified TSP1 protein from activated human platelets (native TSP1) added to BASC/*Tsp1*^{-/-} LuMEC cocultures similarly increased alveolar colony formation as compared to treatment with vehicle alone (Figures S3G and S3H). These data demonstrate that with endothelial cells, TSP1 is sufficient to directly influence BASC alveolar differentiation.

BMP4 Induces BASC Alveolar Differentiation in an Organ-Specific Manner

TSP1 is a multifunctional glycoprotein with numerous receptors; however, control of TSP1 expression is not well understood. We isolated LuMECs at various times after naphthalene or bleomycin injury and analyzed 15 growth factors known to function in lung development or stem cell cultures (Figures S4A–S4D; data not shown). Three factors, *Hgf*, *Tgf- β 1*, and *Bmp4*, showed a similar expression pattern as *Tsp1*; they were downregulated after naphthalene injury and upregulated after bleomycin injury (Figures S4A–S4D and 5A, compare to Figure 4A). To investigate their influence on BASC differentiation, we added recombinant proteins to BASC/LuMEC cocultures. BMP4 treatment led to

the formation of significantly more alveolar colonies and fewer bronchiolar colonies, whereas TGF- β 1 inhibited BASC colony formation, and HGF had no effect (Figures 5B and 5C; data not shown). TSP1 was required for BMP4-induced alveolar differentiation; when BMP4 was added to BASC cocultures with *Tsp1*^{-/-} LuMECs, there was no increase in alveolar colonies (Figures 5B and 5C). BMP4 treatment correlated with activation of Smad1/Smad5 and Erk1/Erk2 signaling and upregulation of *Tsp1* mRNA and protein levels in LuMECs (Figures S4E–S4G, 5D, and 5E). *Tsp1* expression and alveolar differentiation were reduced after treatment with the BMP inhibitor, Noggin (NOG) (Figures 5D, 5E, and S4G). The addition of BMP4 to BASC/LuMEC cocultures did not increase *Tsp1* expression, nor did it increase alveolar colony formation (Figures 5B–5E, S4E, and S4G). Thus, BMP4 treatment specifically induced *Tsp1* in lung endothelial cells.

We recently identified *Tsp1* as a direct target of transcription factor NFATc1 downstream of calcineurin activation (S.R., unpublished data). We asked whether TSP1 induction and BASC differentiation employed the calcineurin-NFAT signaling pathway. Calcineurin is a serine/threonine phosphatase activated by increases in intracellular Ca²⁺; thus, we monitored calcium influx after BMP4 addition using the Ca²⁺ indicator Fluo-4 AM. Within 1 min, BMP4 treatment significantly increased the intensity of Fluo-4 as did VEGF, a known activator of calcineurin signaling (Figure 5F; Movie S1) (Barkauskas et al., 2013; Hesser et al., 2004; Minami et al., 2004). To confirm that BMP4 stimulated NFATc1 activation, NFATc1 localization was assessed by IF. NFATc1 localized to the nucleus in LuMECs within 10 min after BMP4 treatment and was re-exported to the cytoplasm after NOG treatment (Figures 5G and S4H). In contrast, NFATc1 expression and localization were unaltered by BMP4 or NOG in LiMECs (Figure 5G).

Overexpression of a constitutively active NFATc1 (CaNFATc1) or treatment with ionomycin to activate calcineurin in LuMECs strongly induced *Tsp1* expression, indicating that NFATc1 acts upstream of *Tsp1* (Figures 5E and S4H). Furthermore, addition of the specific calcineurin inhibitor, cyclosporin A (CsA), to BASC/LuMEC cocultures significantly abrogated the BMP4-dependent upregulation of *Tsp1* expression and NFATc1 nuclear translocation (Figures 5D, 5E, and 5G). In the presence of CsA

Figure 3. Organ-Specific Endothelial Effects on BASC Differentiation

- (A) Representative images from BASCs cocultured with LuMECs or LiMECs. Arrowhead points to bronchiolar colony, arrow points to alveolar colony, and asterisk indicates bronchioalveolar colony. Scale bars, 500 μ m (top); H&E (middle) and IF (bottom) for CCSP (red), SPC (green), and DAPI (blue). Scale bar, 100 μ m.
- (B) Quantification of colony types from BASCs cocultured with LuMEC or LiMEC. BASC/LiMEC cocultures yielded 3.5-fold increased bronchiolar and 21.5-fold diminished alveolar colony compared to BASC/LuMEC cocultures ($p < 0.001$) (LuMECs, $n = 663$; LiMECs, $n = 627$). n , number of colonies scored. Data presented are the mean of five independent experiments with triplicate wells. Error bars indicate SD (** $p < 0.001$).
- (C) Quantitative real-time PCR for CCSP (black bars) and SPC (white bars) from cocultures. There was a 1.8-fold greater CCSP expression and 19.3-fold less SPC expression in BASC/LiMEC cocultures relative to BASC/LuMEC cocultures ($p < 0.001$). All were normalized to *Gapdh*. Data presented are the mean of three independent experiments with triplicate wells. Error bars indicate SD (** $p < 0.001$).
- (D) Representative results from BASC/LuMEC bronchioalveolar colonies passaged for coculture with LuMECs or LiMECs. GFP images (top) and IF analysis (bottom) for CCSP (red), SPC (green), and DAPI (blue) are shown. Arrowhead points to bronchiolar colony, arrow points to alveolar colony, and asterisk indicates bronchioalveolar colony. Scale bars, 500 μ m (in top) and 100 μ m (in bottom).
- (E) H&E (top) and IF (bottom) analysis for CCSP (red), SPC (green), and DAPI (blue) in tissue sections from subcutaneous coinjection of cells from BASC/LuMEC bronchioalveolar colonies cotransplanted with LuMECs or LiMECs. Scale bars, 100 μ m.
- (F) Quantitative analysis of epithelial structures from (E). Data presented are the mean of two independent experiments with two individual mice wells. Error bars indicate SD (* $p < 0.01$).
- (G) Immunoblotting for TSP1 in LuMECs and LiMECs. *Tsp1*^{-/-} LuMECs were used for negative control. β -actin is the loading control. See also Figure S2.

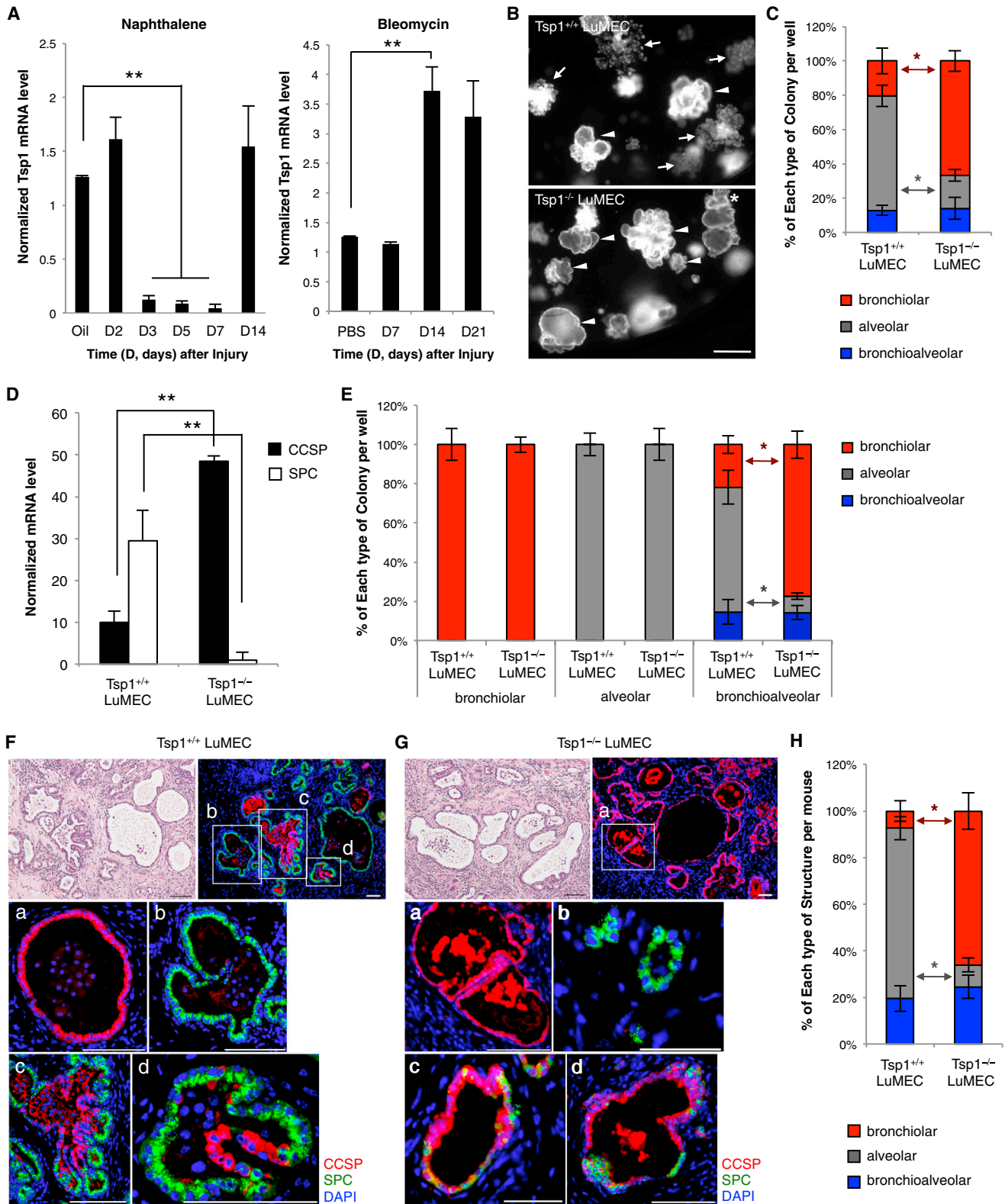


Figure 4. *Tsp1* Deficiency in LuMECs Inhibits Alveolar Differentiation In Vitro and In Vivo

(A) Quantitative real-time PCR for *Tsp1* in LuMECs isolated at indicated time points after naphthalene (left) or bleomycin (right) injury. Corn oil or PBS, diluent controls for naphthalene or bleomycin, respectively, was used. *Tsp1* levels were 10.1-fold less than control during naphthalene injury repair and 2.9-fold higher (legend continued on next page)

and BMP4, BASC/LuMEC cocultures yielded more bronchiolar colonies (Figure 5H). In contrast, BASCs cocultured with CaNFATc1-LuMECs produced significantly more alveolar colonies compared to controls (Figure 5H). CsA did not affect Smad1/Smad5 and Erk1/Erk2 signaling (Figure S4G).

To define BMP4-induced direct interactions of NFATc1 with *Tsp1* in LuMECs, we assessed NFATc1 binding to the *Tsp1* promoter by chromatin immunoprecipitation (ChIP). In BMP4-treated LuMECs but not LiMECs, NFATc1 ChIP showed significant enrichment of *Tsp1* (Figure 5I). Binding of NFATc1 on the *Tsp1* promoter was disrupted in LuMECs treated with BMP4 plus NOG (Figure 5I). These data suggest that, in response to BMP4, NFATc1 activation is sufficient for TSP1-induced BASC alveolar differentiation.

Bmpr1a Is Required for BMP4-Mediated TSP1 Induction in LuMECs

To identify the critical BMP receptor (BMPR) for BMP4-mediated BASC regulation, we tested expression of known BMPRs in LuMECs and found that *Acvr11*, *Bmpr1a*, and *Bmpr2* were highly expressed, whereas *Acvr1*, *Bmpr1b*, *Acvr2a*, or *Acvr2b* showed little or no expression (Figures S5A and S5B). *Bmpr1a* was upregulated in LuMECs, but not in LiMECs, after BMP4 treatment (Figure S5A). These data, and previous work linking *Bmpr1a* and NFATc1 to regulation of hair follicle stem cells (Horsley et al., 2008), prompted us to further examine *Bmpr1a* in BASC differentiation.

To test the role of *Bmpr1a* in BASC/LuMEC cocultures, LuMECs were isolated from *Bmpr1a^{fl/fl}* mice followed by infection with adenovirus-empty vector (Ad-Emp) or adenovirus-Cre recombinase (Ad-Cre). Loss of *Bmpr1a* expression was confirmed by quantitative real-time PCR (Figure 6A). BASCs cocultured with *Bmpr1a*-depleted LuMECs showed impaired alveolar differentiation; BASC/*Bmpr1a^{fl/fl}*; Ad-Cre LuMEC produced 4.6-fold more bronchiolar colonies and 1.4-fold fewer alveolar colonies than controls (Figure 6B). *Bmpr1a* deficiency led to 2.42-fold less *Tsp1* mRNA in Cre-treated *Bmpr1a^{fl/fl}* LuMECs than controls and reduced *Tsp1* induction up to 12 hr after BMP4 treatment (Figures 6C and 6D). Finally, BMP4-induced nuclear translocation of NFATc1 was impaired in *Bmpr1a*-depleted LuMECs (Fig-

ure 6E). These data supported a model whereby BMP4 activates calcineurin/NFATc1 signaling through *Bmpr1a* to induce TSP1 expression in LuMECs.

Given its role in BASC differentiation, we asked whether *Bmpr1a* also played a role in lung injury repair. *Bmpr1a* expression levels were assayed in LuMECs at various time points following naphthalene and bleomycin injury. Although there was no remarkable change after naphthalene, a significant increase in *Bmpr1a* expression (4.8-fold; $p < 0.01$) was seen at 14 days following bleomycin treatment (Figure 6F). Changes in Bmp signaling were also observed during lung epithelial regeneration; phosphorylated Smad1/Smad5 and Erk1/Erk2 were detected in LuMECs from uninjured mice and during bleomycin injury repair, whereas these phosphorylated proteins were decreased during naphthalene injury repair and undetectable in LiMECs (Figures S5C and S5D).

We probed epithelial cells as a source of BMP4 after lung injury and found that in homeostatic conditions, *Bmp4* expression was higher in AT2 cells and BASCs compared to total lung cells (Figure 6G). Three days after naphthalene treatment, *Bmp4* expression was downregulated in AT2 cells and BASCs, returning to baseline 14 days after injury (Figure 6G). In contrast, BASCs expressed 2.7-fold higher levels of *Bmp4* 14 days after bleomycin compared to controls ($p < 0.01$), and AT2 cells showed 1.5-fold increased *Bmp4* expression 21 days after bleomycin ($p < 0.01$ versus PBS) (Figure 6G). These results suggest that alveolar injury triggers *Bmp4* induction in BASCs, AT2 cells, or other epithelial cells, subsequently upregulating *Tsp1* from lung endothelial cells to control BASC differentiation in a *Bmpr1a*-calcineurin-NFATc1-dependent manner.

Altered Bronchiolar and Alveolar Injury Repair in *Tsp1* Null Mice

Our studies identify TSP1 as a key regulator of lung stem cell differentiation; thus, we tested the effects of *Tsp1* deficiency on bronchiolar epithelial repair. We first confirmed that *Tsp1^{-/-}* mice (Lawler et al., 1998) did not exhibit a lung phenotype without injury (Figure S6A). IF analysis confirmed sufficient club cell ablation in *Tsp1^{+/+}* and *Tsp1^{-/-}* mice 2 days after naphthalene treatment (Figures 7A and 7B). Club cell numbers remained

than control during bleomycin injury repair ($p < 0.001$). All were normalized to *Gapdh*. Data presented are the mean of samples from three individual mice. Error bars indicate SD (** $p < 0.001$).

(B) Representative GFP images of BASCs cocultured with *Tsp1^{+/+}* (top) or *Tsp1^{-/-}* LuMECs (bottom). Arrowhead points to bronchiolar colony, arrow points to alveolar colony, and the asterisk indicates bronchioalveolar colony. Scale bar, 500 μ m.

(C) Quantification of colony types from BASCs cocultured with *Tsp1^{+/+}* or *Tsp1^{-/-}* LuMECs ($n = 605$ and 753 , respectively). n , number of colonies scored. Data presented are the mean of five independent experiments with triplicate wells. Error bars indicate SD (* $p < 0.01$).

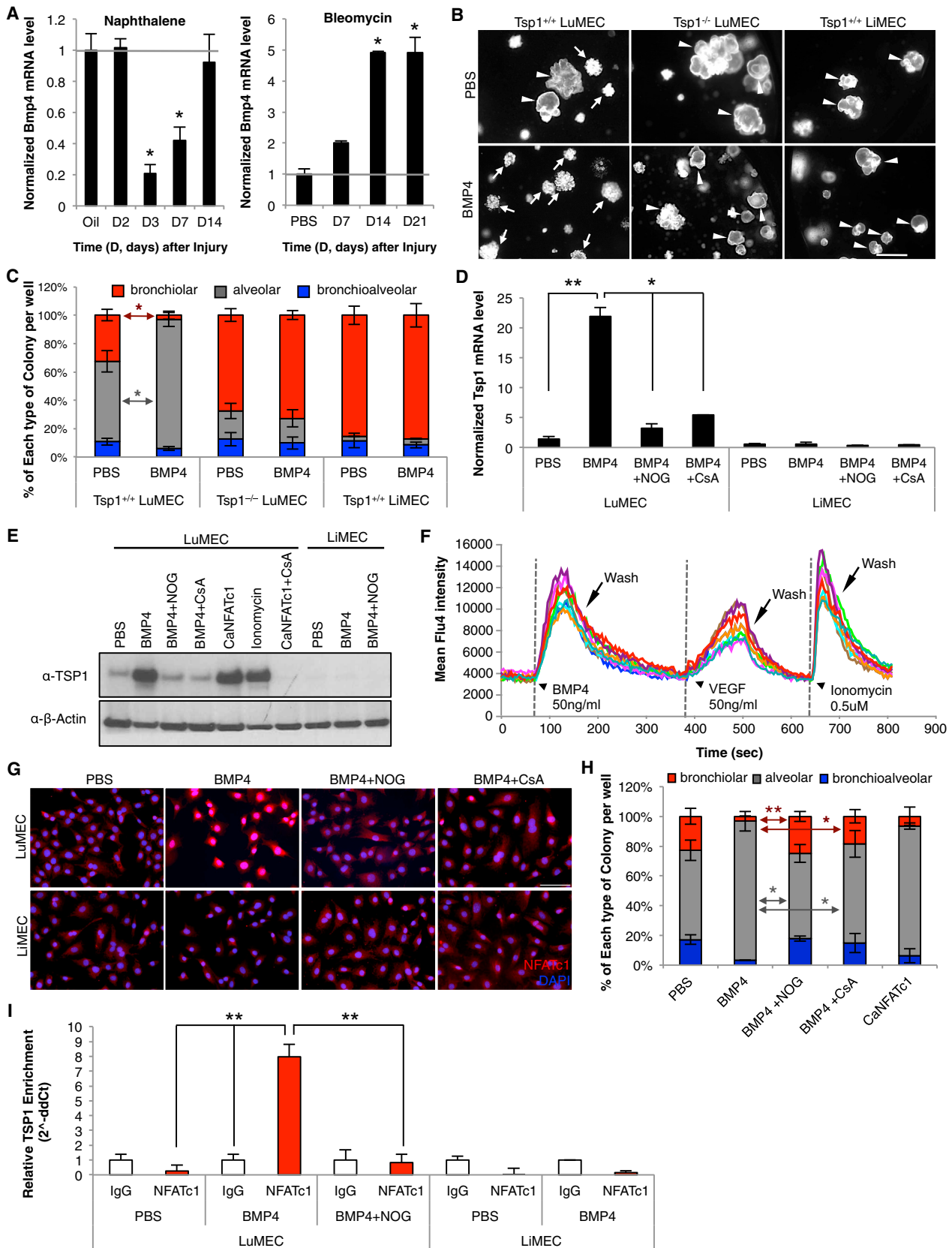
(D) Quantitative real-time PCR analysis for SPC and CCSP from colonies as in (B). There were 4.8-fold higher levels of CCSP expression and 29.5-fold less SPC expression in BASC/*Tsp1^{-/-}* LuMEC cocultures versus BASC/*Tsp1^{+/+}* LuMEC cocultures ($p < 0.001$). All were normalized to *Gapdh*. Data presented are the mean of three independent experiments with triplicate wells. Error bars indicate SD (** $p < 0.001$).

(E) Quantification of colony types from passaged colonies cocultured with *Tsp1^{+/+}* or *Tsp1^{-/-}* LuMECs: bronchiolar, $n = 471$ in *Tsp1^{+/+}* and $n = 633$ in *Tsp1^{-/-}*; alveolar, $n = 460$ in *Tsp1^{+/+}* and $n = 532$ in *Tsp1^{-/-}*; and bronchioalveolar, $n = 566$ in *Tsp1^{+/+}* and $n = 651$ in *Tsp1^{-/-}*. Cells from bronchioalveolar colonies cocultured with *Tsp1^{-/-}* LuMECs produced 3.6-fold more bronchiolar colonies and 5.7-fold less alveolar colonies ($p < 0.01$), respectively, than cocultures with *Tsp1^{+/+}* LuMECs. n , number of colonies scored. Data presented are the mean of four independent experiments with duplicate wells of five individual colonies. Error bars indicate SD (* $p < 0.01$).

(F and G) H&E (top left) and IF analysis for CCSP (red), SPC (green), and DAPI (blue) in tissue sections from subcutaneous coinjection of bronchioalveolar colonies with *Tsp1^{+/+}* (F) or *Tsp1^{-/-}* LuMECs (G). Insets (top right) show high-power view (a, bronchiolar; b, alveolar; c and d, bronchioalveolar). Scale bars, 100 μ m.

(H) Quantitative analysis of epithelial structures from (F) and (G). Data presented are the mean of two independent experiments with three individual mice. Error bars indicate SD (* $p < 0.01$).

See also Figure S3.



(legend on next page)

low 5–7 days after naphthalene in *Tsp1*^{+/+} mice, whereas *Tsp1*^{-/-} mice exhibited significantly more club cells at these time points (Figures 7A and 7B). Interestingly, the number of BASCs peaked earlier in *Tsp1*^{-/-} mice in response to naphthalene (Figure 7C).

Intratracheal administration of bleomycin selectively ablates AT2 cells (Aso et al., 1976); thus, we evaluated the requirement for TSP1 during alveolar injury repair. IF analysis revealed a 4.4-fold reduction in SPC-expressing AT2 cells after bleomycin treatment in *Tsp1*^{-/-} mice (Figures 7D and 7E). Numerous bromodeoxyuridine (BrdU)-labeled AT2 cells were observed in wild-type mice, yet *Tsp1*^{-/-} mice had fewer BrdU-positive cells (Figure 7D). A slight yet significant increase in fibrosis was seen in *Tsp1*^{-/-} mice compared to wild-type mice (Figures 7F and S6B), consistent with previous reports (Ezzie et al., 2011). The number of BASCs in *Tsp1*^{+/+} mice increased 14 days after injury and declined to baseline after 28 days (Figures 7G and 7H), as expected (Kim et al., 2005). However, *Tsp1*^{-/-} mice showed increased numbers of BASCs through 28 days after injury (Figures 7G and 7H). These data demonstrate a defect in alveolar epithelial repair in *Tsp1* deficiency and suggest that BASCs failed to sufficiently differentiate in response to alveolar injury.

We examined the sufficiency of endothelial-derived TSP1 for BASC alveolar differentiation following bleomycin injury. Conditioned medium (CM) collected from wild-type LuMECs, wild-type LiMECs, or *Tsp1*^{-/-} LuMECs (Figure S6C) was administered following bleomycin treatment. *Tsp1* null mice treated with wild-type LuMEC CM exhibited AT2 cell regeneration comparable to wild-type mice; a 3-fold increase in SPC-positive cells was observed in CM- versus media-treated *Tsp1* null mice (Figures S6D and S6E). Neither CM from *Tsp1*^{-/-} LuMECs nor CM from wild-type LiMECs facilitated AT2 cell regeneration in *Tsp1*^{-/-} mice (Figures S6D and S6E). CM from wild-type

LuMECs also reduced fibrosis in *Tsp1* null mice (Figure S6F) and restored BASC numbers comparable to those in wild-type mice (Figures S6G and S6H). Taken together, LuMEC-derived TSP1 was sufficient for the repair of alveolar epithelial injury via regulation of BASC differentiation.

DISCUSSION

We have defined a signaling pathway that specifies lung stem cell differentiation. Endothelial cells supported BASC differentiation into multiple epithelial lineages in vitro and after subcutaneous injection. Using these 3D platforms, we identified a BMP4-controlled NFATc1-TSP1 axis in lung endothelial cells that directs BASC differentiation to the alveolar lineage. This endothelial-epithelial crosstalk is one mechanism by which lung stem cell differentiation choices are regulated in response to lung injury in vivo.

The differentiation capacity we uncovered in endothelial cell-supported 3D cocultures and cotransplantations strengthens the stem cell identity of BASCs. Single FACS-purified BASCs were capable of multilineage differentiation. The degree to which these cells represent dual-positive CCSP/SPC cells in vivo remains an outstanding question. Further interrogation using in vivo systems to specifically label BASCs in their microenvironment remains an important goal. This work and previous studies provide evidence that distinguishes BASCs from other lung stem/progenitors, making it unlikely that other cell populations contributed to our findings: basal cells from the upper airways do not require stromal cells for growth in 3D cultures (Rock et al., 2009), Sca1-low bronchiolar stem cells do not produce cells with alveolar phenotypes (Teisanu et al., 2011), and the SPC-negative integrin- α 6 β 4-positive progenitors may be restricted to alveolar lineages (Chapman et al., 2011). Direct comparisons of BASCs with other lung stem/progenitor populations could

Figure 5. BMP4-Induced, NFATc1-Dependent *Tsp1* Expression in LuMECs Is Required for BASC Alveolar Differentiation

(A) Quantitative real-time PCR for *Bmp4* from LuMECs isolated at indicated time points after naphthalene (left) or bleomycin (right) injury. All were normalized to *Gapdh*, and expression in controls is set to one (1) for comparison. Data presented are the mean of samples from three individual mice. Error bars indicate SD (**p* < 0.01).
 (B) Representative GFP images of BASC cocultures treated with PBS or BMP4 (50 ng/ml). BASC 3D cocultures with *Tsp1*^{+/+} LuMEC (left), *Tsp1*^{-/-} LuMEC (middle), or LiMEC (right) are shown. Arrowhead points to bronchiolar colony, and arrow points to alveolar colony. Scale bar, 500 μ m.
 (C) Quantification of colony types from BASC cocultures treated with PBS or BMP4 with *Tsp1*^{+/+} LuMEC (*n* = 414, PBS; *n* = 367, BMP4), *Tsp1*^{-/-} LuMEC (*n* = 498, PBS; *n* = 425, BMP4), or *Tsp1*^{+/+} LiMEC (*n* = 376, PBS; *n* = 334, BMP4). BASC/*Tsp1*^{+/+} LuMEC cocultures with BMP4 treatment showed 1.6-fold more alveolar colonies than PBS control (*p* < 0.01) and 3.0-fold less bronchiolar colonies than control (*p* < 0.01). *n*, number of colonies scored. Data presented are the mean of three independent experiments with triplicate wells. Error bars indicate SD (**p* < 0.01).
 (D) Quantitative real-time PCR for *Tsp1* in LuMECs isolated by FACS (GFP negative) after coculture with BASCs in the presence of PBS control, BMP4, BMP4 plus NOG, or BMP4 plus CsA. BMP4 treatment increased *Tsp1* levels in LuMECs by 15.5-fold greater than PBS control (*p* < 0.001). All were normalized to *Gapdh*. Data presented are the mean of three independent experiments with triplicate wells. Error bars indicate SD (**p* < 0.01; ***p* < 0.001).
 (E) Immunoblotting for TSP1 in LuMECs treated as indicated. CaNFATc1, LuMEC infected with constitutively active form of NFATc1. β -actin is the loading control.
 (F) Intracellular calcium measurement. BMP4, VEGF, or ionomycin was loaded at the indicated time (arrowhead) followed by washing (arrow). Induced calcium mobilization was monitored by Fluo-4.
 (G) IF analysis for NFATc1 (red) and DAPI (blue) in LuMEC cultures treated as in (E). Scale bar, 100 μ m.
 (H) Quantification of colony types from passage of BASC/LuMEC bronchioalveolar colonies treated with PBS (*n* = 415), BMP4 (*n* = 385), BMP4 plus NOG (*n* = 371), or BMP4 plus CsA (*n* = 392) or cocultured with CaNFATc1-LuMECs (*n* = 388). Alveolar colony formation was 1.6-fold less in BMP4-treated cultures with NOG (*p* < 0.01) and 1.4-fold less with CsA (*p* < 0.01). Bronchiolar colony formation with BMP4 was increased 7.8-fold (*p* < 0.001) with NOG and 5.6-fold greater after CsA (*p* < 0.01). BASC/CaNFATc1-LuMEC cocultures formed 1.5-fold more alveolar colonies (*p* < 0.01) and 3.5-fold less bronchiolar colonies (*p* < 0.001) compared to BASC/LuMEC. *n*, number of colonies scored. Data presented are the mean of three independent experiments with five individual colonies. Error bars indicate SD (**p* < 0.01; ***p* < 0.001).
 (I) Quantitative real-time PCR using *Tsp1* promoter primers and DNA purified from NFATc1-ChIP in LuMECs after treatments indicated for 30 min. NFATc1 ChIP in LuMECs with BMP4 addition showed 8-fold greater *Tsp1* enrichment than IgG control and 30.8-fold greater than PBS control (*p* < 0.001). The enrichment relative to *Gapdh* is shown. Data presented are the mean of three independent experiments with triplicate wells. Error bars indicate SEM (***p* < 0.001).
 See also Figure S4.

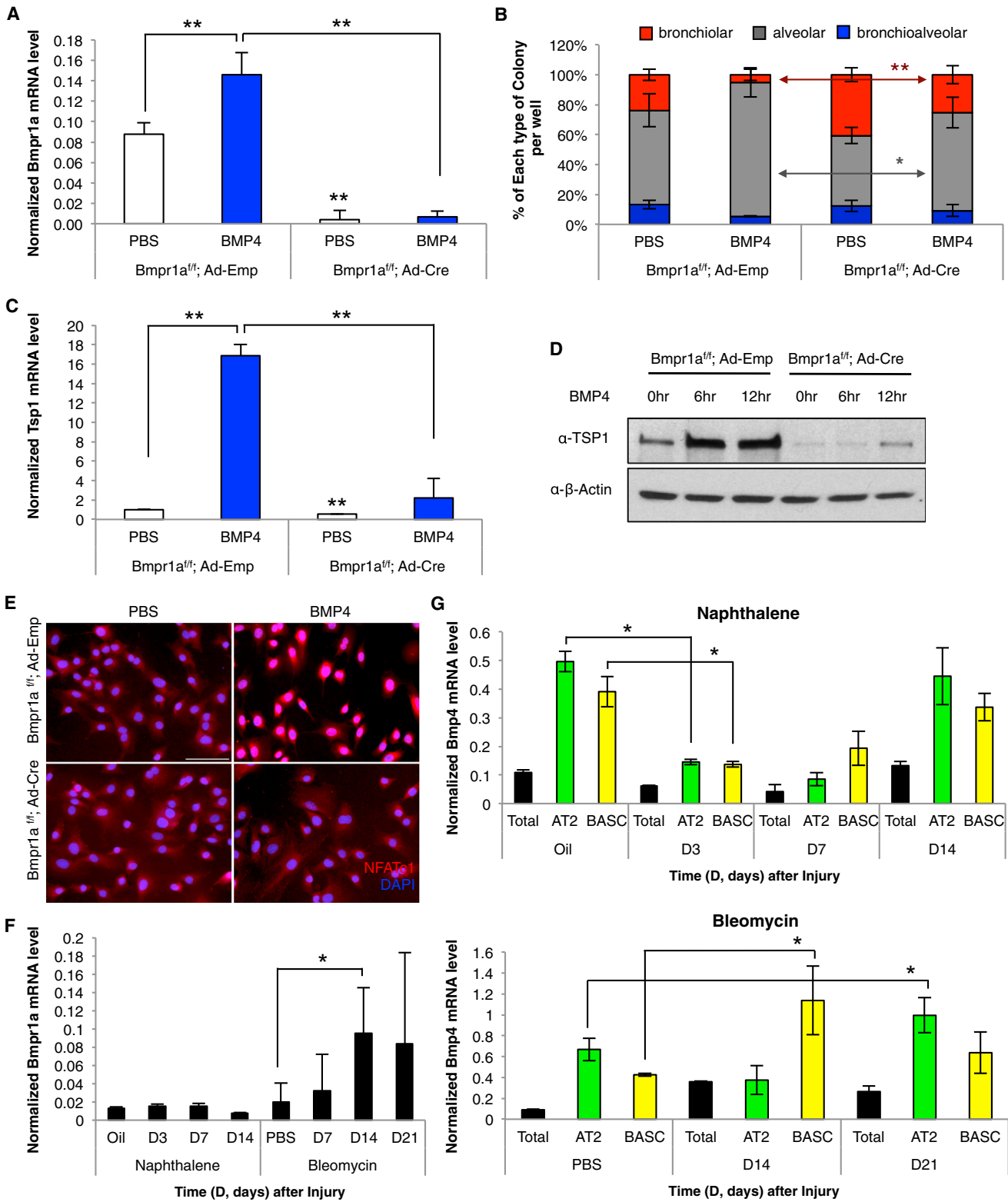


Figure 6. *Bmpr1a* Is Required for BASC Alveolar Differentiation

(A) Quantitative real-time PCR for *Bmpr1a* in *Bmpr1a^{fl/fl}*; Ad-Emp or *Bmpr1a^{fl/fl}*; Ad-Cre LuMECs isolated from coculture with BASCs with (blue bars) or without BMP4 (white bars). All were normalized to *Gapdh*. Data presented are the mean of three independent experiments with triplicate wells. Error bars indicate SD (***p* < 0.001).

(legend continued on next page)

reveal that the BMP4-NFATc1-TSP1 signaling axis is broadly important for differentiation control in the distal lung.

Our results suggest that a BMP4-NFATc1-TSP1 signaling axis operates among stem cells, epithelial cells, and endothelial cells to repair lineage-specific injury in an organ-specific context. Our data and previous reports lead us to hypothesize that the lung epithelial injury repair signaling cascade begins with sensing changes in BMP4 and/or other additional molecules expressed by BASCs and distal lung epithelial cells (Masterson et al., 2011; Rosendahl et al., 2002; Sountoulidis et al., 2012). BMP4 appears to primarily act in lung endothelial cells by stimulating calcineurin and altering NFATc1 localization. Phosphorylation of SMAD1/SMAD5 and ERK1/ERK2 and increased *Nfatc1* transcript were also detected after BMP4 treatment in vitro and in vivo, suggesting that canonical Bmp transcriptional responses also play a role in this setting. *Tsp1* expression is upregulated then secreted by lung endothelial cells signaling back to BASCs. It remains to be determined which TSP1 receptors and downstream signaling molecules regulate alveolar differentiation. The role of Tsp1 in lung injury repair may also involve interactions between other cell types aside from endothelial cells, and other endothelial factors or a structural role from endothelia may also be critical. Finally, in the absence of a known human BASC equivalent, it is unknown whether a BMP4-NFATc1-TSP1 pathway operates in human lungs.

This work reveals that manipulation of the microenvironment can direct the lineage-specific differentiation of lung stem cells, an important proof of principle for therapeutic development for lung diseases. Whereas seminal strides have been made to differentiate induced pluripotent stem cells into lung cells (Green et al., 2011; Longmire et al., 2012; Mou et al., 2012), directed differentiation to produce a specific lung epithelial lineage is not yet possible. Our work identifies molecules, such as TSP1, that could be used to specify alveolar epithelial differentiation from adult multipotent stem cells. We and others have begun to identify key differences between organ-specific endothelia that may reveal additional molecules for differentiation control (Nolan et al., 2013). Injured or depleted lung epithelial cells are the hallmark of numerous pulmonary diseases, including alveolar damage in pulmonary fibrosis and bronchiolar ablation in bronchiolitis obliterans. Drugs that promote the relevant lineage-specific differentiation activity of lung stem cells might be useful in stimulating the repair of patients' damaged lung cells. For example, drugs driving alveolar differentiation might aid patients with fibrosis, whereas chemicals promoting bronchiolar differentiation may help those patients with bronchiolitis obliterans. The organ-specific BMP4-NFATc1-TSP1 axis in lung endothelial

cells we defined could be a therapeutic avenue for these and other numerous lung diseases. Further elucidation of the networks that regulate BASCs could identify new potential drug targets for lung disease in stem cells and their interacting niche including endothelial cells.

EXPERIMENTAL PROCEDURES

All mice work was approved by the CHB Animal Care and Use Committee, accredited by AAALAC, and was performed in accordance with relevant institutional and national guidelines and regulations.

Endothelial Cell Preparation

LuMECs and LiMECs were isolated from 2- to 4-week-old mice by negative selection with anti-CD45-conjugated magnetic beads and positive selection with anti-CD31-conjugated magnetic beads. CD31-positive cells were then amplified in a gelatin-coated culture plate for 3–5 days followed by reselection with anti-CD31-conjugated magnetic beads. Endothelial cell purity was determined by IF staining for CD31, VE-Cadherin, and VEGFR2, and cells were used for experiments between passages 2 and 6. For Ac-LDL uptake, endothelial cells were incubated with 10 $\mu\text{g/ml}$ Dil-ac-LDL for 2 hr at 37°C followed by staining with DAPI. For Matrigel tube formation, endothelial cells were seeded on Matrigel-coated 24-well plates (1×10^5 cells/well), incubated for 1 hr at 37°C, and added fresh medium. One to 3 days after plating, tube formation was observed.

3D Cocultures and Cotransplantation

Amplified LuMECs/LiMECs were used for 3D cocultures or cotransplantations of AT2 cells and BASCs or dissociated colonies from BASCs. AT2 cells and BASCs were isolated from 7- to 10-week-old mice by FACS using pan-CD45-APC, CD31-APC, Sca1 (Ly-6A/E)-APC-Cy7, EpCAM-PE-Cy7 with DAPI staining. Freshly isolated cells were mixed with growth-factor-reduced Matrigel containing LuMECs or LiMECs, and the cell mixtures were plated in transwell plates or transplanted via subcutaneous injection into nude mice. For cocultures/cotransplantation of individual colonies, similar-sized individual colonies were picked under the fluorescence microscope after enzymic digestion. Picked individual colonies were further trypsinized into single cells for quantitative real-time PCR, passaged for subsequent colony formation, or transplanted by subcutaneous injection with LuMECs/LiMECs. For "helper cell" 3D single-cell cultures, freshly isolated EpCAM-positive lung epithelial cells were irradiated (26 Gy), and 50,000 cells were resuspended with LuMECs/Matrigel and a single BASC or AT2 cell. For serial passages, day 14 AT2 cell or BASC 3D cocultures were dissociated to generate a single-cell suspension followed by FACS for GFP. GFP+ cells were resuspended in fresh LuMEC/Matrigel mixtures. Media for 3D cocultures were replaced every other day with supplements for up to 14–21 days. Mice coinjected with cells/Matrigel were euthanized 4 weeks after injection for analysis of histopathology.

Preparation of TSP1

Blood was collected from 6- to 8-week-old mice by retro-orbital bleeding and centrifuged to separate platelets that were activated by incubation with 1 U of thrombin for 20 min at 37°C. Releasate was then obtained by centrifugation to obtain TSP1. Releasate was added to 3D coculture of BASCs every other day.

(B) Quantification of colony types from BASC cocultures treated with PBS or BMP4 with Ad-Emp LuMECs ($n = 423$, PBS; $n = 388$, BMP4) or Ad-Cre LuMECs ($n = 456$, PBS; $n = 441$, BMP4). After BMP4 treatment, whereas BASC/Ad-Emp LuMEC generated 3.8-fold less bronchiolar colonies ($p < 0.001$) and 1.4-fold more alveolar colonies ($p < 0.01$) compared to PBS controls, BASC/Ad-Cre LuMEC produced bronchiolar and alveolar colonies comparable to PBS controls. n , number of colonies scored. Data presented are the mean of three independent experiments with triplicate wells. Error bars indicate SD ($*p < 0.01$; $**p < 0.001$).

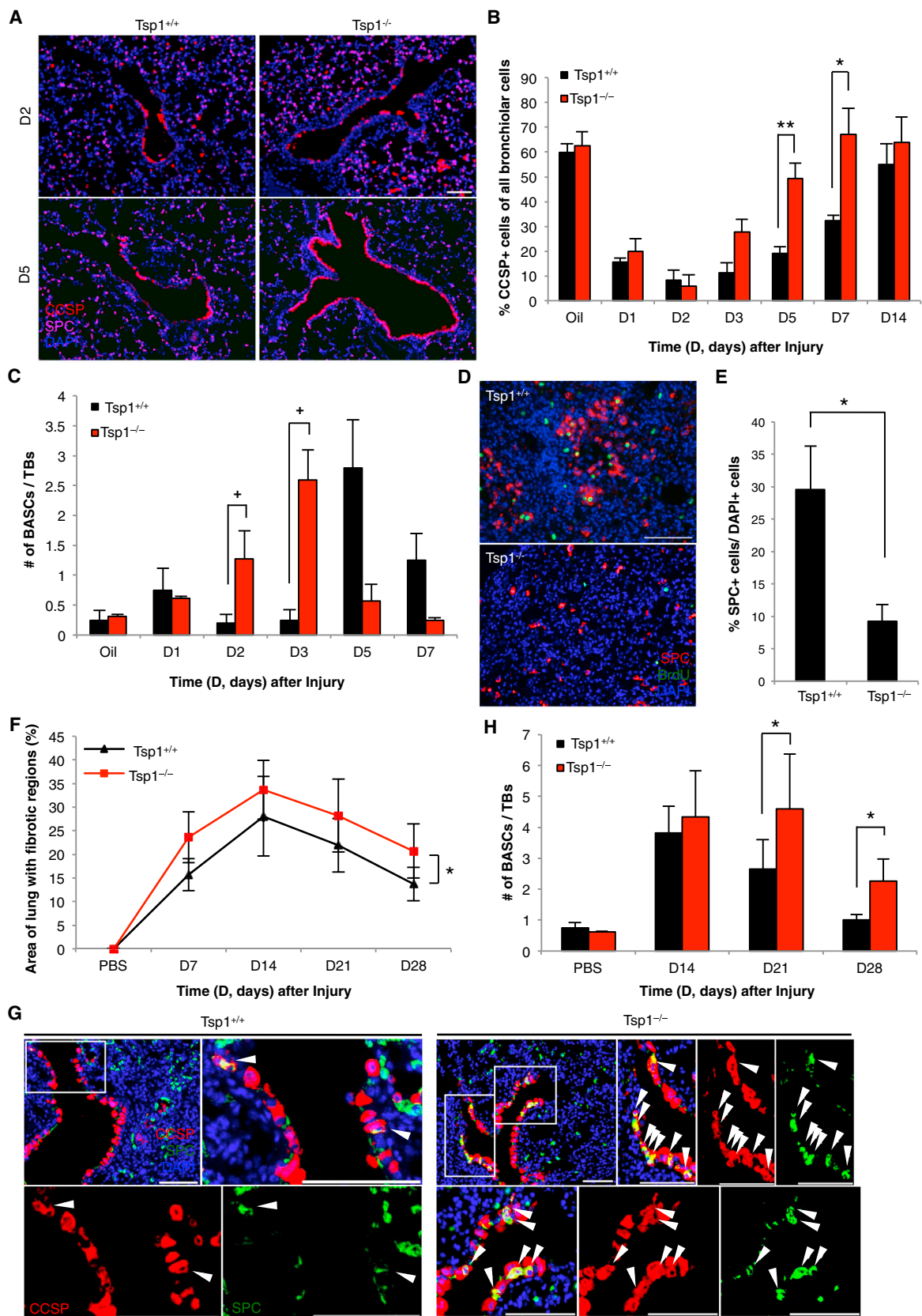
(C) Quantitative real-time PCR for *Tsp1* as in (A).

(D) Immunoblotting for TSP1 in *Bmpr1a^{fl/fl}*; Ad-Emp or *Bmpr1a^{fl/fl}*; Ad-Cre LuMECs at indicated time points after BMP4 treatment. β -actin is the loading control.

(E) IF analysis for NFATc1 (red) and DAPI (blue) in Ad-Emp or Ad-Cre LuMEC cultures treated with PBS or BMP4. Scale bar, 100 μm .

(F and G) Quantitative real-time PCR for *Bmpr1a* (black bars) from LuMECs (F) or *Bmp4* from AT2 cells (green bars), BASCs (yellow bars) or total live lung cells (black bars) (G) isolated at indicated time points after naphthalene (G, top) or bleomycin (G, bottom). All were normalized to *Gapdh*. Data presented are the mean of samples from three independent mice. Error bars indicate SD ($*p < 0.01$).

See also Figure S5.



(legend on next page)

Lung Injury

In vivo lung injury experiments were conducted in 7- to 10-week-old mice that received naphthalene (275 mg/kg) via intraperitoneal injection or bleomycin (0.035 U/mice) via intratracheal injection. CMs were collected from LuMECs/LiMECs that were incubated in serum-free media for 24 hr following 10-fold concentration. CM was administered via tail vein injection at a volume of 100 μ l every other day for 21 days after bleomycin injection.

ChIP

ChIP assay was performed with LuMECs/LiMECs that were incubated with serum-free media overnight and were treated with BMP4 (50 ng/ml) or BMP4 (50 ng/ml) plus NOG (100 ng/ml) for 30 min. After crosslinking, the sonicated lysate was employed to immunoprecipitation using anti-NFATc1 or anti-mouse IgG with a mix of protein A/G beads.

SUPPLEMENTAL INFORMATION

Supplemental Information includes Extended Experimental Procedures, six figures, and one movie and can be found with this article online at <http://dx.doi.org/10.1016/j.cell.2013.12.039>.

ACKNOWLEDGMENTS

We thank the BCH FACS facility, members of the C.F.K. lab, L. Zon, D. Scadden, P. Oh, C. Han, C. Fillmore, K. Townsend, G. Evans, and J. Sage for technical assistance and/or helpful discussions, and R. Bronson for histopathology. This work was supported by the Hope Funds for Cancer Research (JHL), R01 CA118374 (to S.R.), R01 DK077097 (to Y.-H.T.), U01 HL100402 and 1U01HL099997 under NHLBI RFA-HL-09-004 (to C.F.K., B.R.S., and A.J.W.), the Harvard Stem Cell Institute (to Y.-H.T. and C.F.K.), the Foundation Leducq (to K.D.B.), and RO1 HL090136, American Cancer Society Research Scholar Grant RSG-08-082-01-MGO, and a Basil O'Connor March of Dimes Starter Award (to C.F.K.). This research was funded by Alfred A. and Gilda K. Slifka (to C.F.K.).

Received: May 8, 2013

Revised: October 24, 2013

Accepted: December 27, 2013

Published: January 30, 2014

REFERENCES

Adams, J.C., and Lawler, J. (2004). The thrombospondins. *Int. J. Biochem. Cell Biol.* 36, 961–968.

Aso, Y., Yoneda, K., and Kikkawa, Y. (1976). Morphologic and biochemical study of pulmonary changes induced by bleomycin in mice. *Lab. Invest.* 35, 558–568.

Baenziger, N.L., Brodie, G.N., and Majerus, P.W. (1971). A thrombin-sensitive protein of human platelet membranes. *Proc. Natl. Acad. Sci. USA* 68, 240–243.

Barkauskas, C.E., Crouse, M.J., Rackley, C.R., Bowie, E.J., Keene, D.R., Stripp, B.R., Randell, S.H., Noble, P.W., and Hogan, B.L. (2013). Type 2 alveolar cells are stem cells in adult lung. *J. Clin. Invest.* 123, 3025–3036.

Chapman, H.A., Li, X., Alexander, J.P., Brumwell, A., Lorizio, W., Tan, K., Sonnenberg, A., Wei, Y., and Vu, T.H. (2011). Integrin α 6 β 4 identifies an adult distal lung epithelial population with regenerative potential in mice. *J. Clin. Invest.* 121, 2855–2862.

Chen, H., Herndon, M.E., and Lawler, J. (2000). The cell biology of thrombospondin-1. *Matrix Biol.* 19, 597–614.

DeLisser, H.M., Helmke, B.P., Cao, G., Egan, P.M., Taichman, D., Fehrenbach, M., Zaman, A., Cui, Z., Mohan, G.S., Baldwin, H.S., et al. (2006). Loss of PECAM-1 function impairs alveolarization. *J. Biol. Chem.* 281, 8724–8731.

Ding, B.S., Nolan, D.J., Guo, P., Babazadeh, A.O., Cao, Z., Rosenwaks, Z., Crystal, R.G., Simons, M., Sato, T.N., Worgall, S., et al. (2011). Endothelial-derived angiocrine signals induce and sustain regenerative lung alveolarization. *Cell* 147, 539–553.

Dovey, J.S., Zacharek, S.J., Kim, C.F., and Lees, J.A. (2008). Bmi1 is critical for lung tumorigenesis and bronchioalveolar stem cell expansion. *Proc. Natl. Acad. Sci. USA* 105, 11857–11862.

Ezzie, M.E., Piper, M.G., Montague, C., Newland, C.A., Opalek, J.M., Baran, C., Ali, N., Brigstock, D., Lawler, J., and Marsh, C.B. (2011). Thrombospondin-1-deficient mice are not protected from bleomycin-induced pulmonary fibrosis. *Am. J. Respir. Cell Mol. Biol.* 44, 556–561.

Ganguly, P. (1971). Isolation and properties of a thrombin-sensitive protein from human blood platelets. *J. Biol. Chem.* 246, 4286–4290.

Green, M.D., Chen, A., Nostro, M.C., d'Souza, S.L., Schaniel, C., Lemischka, I.R., Gouon-Evans, V., Keller, G., and Snoeck, H.W. (2011). Generation of anterior foregut endoderm from human embryonic and induced pluripotent stem cells. *Nat. Biotechnol.* 29, 267–272.

Hesser, B.A., Liang, X.H., Camenisch, G., Yang, S., Lewin, D.A., Scheller, R., Ferrara, N., and Gerber, H.P. (2004). Down syndrome critical region protein 1 (DSCR1), a novel VEGF target gene that regulates expression of inflammatory markers on activated endothelial cells. *Blood* 104, 149–158.

Horsley, V., Aliprantis, A.O., Polak, L., Glimcher, L.H., and Fuchs, E. (2008). NFATc1 balances quiescence and proliferation of skin stem cells. *Cell* 132, 299–310.

Iruela-Arispe, M.L., Liska, D.J., Sage, E.H., and Bornstein, P. (1993). Differential expression of thrombospondin 1, 2, and 3 during murine development. *Dev. Dyn.* 197, 40–56.

Jakkula, M., Le Cras, T.D., Gebb, S., Hirth, K.P., Tuder, R.M., Voelkel, N.F., and Abman, S.H. (2000). Inhibition of angiogenesis decreases alveolarization in the developing rat lung. *Am. J. Physiol. Lung Cell. Mol. Physiol.* 279, L600–L607.

Figure 7. Accelerated Bronchiolar Injury Repair and Impaired Alveolar Injury Repair in *Tsp1* Null Mice

(A) Representative images showing club cell injury or repair determined by IF for CCSP (red), SPC (purple), and DAPI (blue) in lung tissue sections from *Tsp1*^{+/+} and *Tsp1*^{-/-} mice at 2 days (top) or 5 days (bottom) after naphthalene.

(B and C) Quantification of naphthalene injury repair in *Tsp1*^{+/+} (black bars) and *Tsp1*^{-/-} (red bars) lungs.

(B) For club cells, the percentage of DAPI-positive, CCSP-positive bronchiolar cells was assessed at indicated time points (*p < 0.01; **p < 0.001).

(C) The numbers of CCSP-positive, SPC-positive BASCs in terminal bronchioles (TBs) were counted at indicated time points (+p < 0.05).

(D) Representative IF analysis for SPC (red), BrdU (green), and DAPI (blue) in fibrotic lung regions from *Tsp1*^{+/+} or *Tsp1*^{-/-} mice 21 days postintratracheal bleomycin injection.

(E and F) Quantification of bleomycin injury repair.

(E) The percentage of DAPI-positive, SPC-positive cells 21 days after bleomycin is shown (*p < 0.01).

(F) The area of lung with fibrotic regions at each time point shown was calculated as the percentage of total lung area with fibrosis (*p < 0.01).

(G) Representative IF analysis for CCSP (red), SPC (green), and DAPI (blue) in terminal bronchioles 21 days after bleomycin showing BASCs (arrowheads) in *Tsp1*^{+/+} (left) and *Tsp1*^{-/-} mice (right). Scale bars, 100 μ m.

(H) Quantification of BASCs as in (C) during bleomycin injury repair in *Tsp1*^{+/+} (black bars) and *Tsp1*^{-/-} mice (red bars). Data presented are the mean of three individual mice. Error bars indicate SD (*p < 0.01).

See also Figure S6.

- Jones, D.L., and Wagers, A.J. (2008). No place like home: anatomy and function of the stem cell niche. *Nat. Rev. Mol. Cell Biol.* 9, 11–21.
- Kim, C.F., Jackson, E.L., Woolfenden, A.E., Lawrence, S., Babar, I., Vogel, S., Crowley, D., Bronson, R.T., and Jacks, T. (2005). Identification of bronchioalveolar stem cells in normal lung and lung cancer. *Cell* 121, 823–835.
- Lawler, J. (2002). Thrombospondin-1 as an endogenous inhibitor of angiogenesis and tumor growth. *J. Cell. Mol. Med.* 6, 1–12.
- Lawler, J.W., Slayter, H.S., and Coligan, J.E. (1978). Isolation and characterization of a high molecular weight glycoprotein from human blood platelets. *J. Biol. Chem.* 253, 8609–8616.
- Lawler, J., Sunday, M., Thibert, V., Duquette, M., George, E.L., Rayburn, H., and Hynes, R.O. (1998). Thrombospondin-1 is required for normal murine pulmonary homeostasis and its absence causes pneumonia. *J. Clin. Invest.* 101, 982–992.
- Lee, J.H., Kim, J., Gludish, D., Roach, R.R., Saunders, A.H., Barrios, J., Woo, A.J., Chen, H., Conner, D.A., Fujiwara, Y., et al. (2013). Surfactant protein-C chromatin-bound green fluorescence protein reporter mice reveal heterogeneity of surfactant protein C-expressing lung cells. *Am. J. Respir. Cell Mol. Biol.* 48, 288–298.
- Longmire, T.A., Ikononou, L., Hawkins, F., Christodoulou, C., Cao, Y., Jean, J.C., Kwok, L.W., Mou, H., Rajagopal, J., Shen, S.S., et al. (2012). Efficient derivation of purified lung and thyroid progenitors from embryonic stem cells. *Cell Stem Cell* 10, 398–411.
- Masterson, J.C., Molloy, E.L., Gilbert, J.L., McCormack, N., Adams, A., and O’Dea, S. (2011). Bone morphogenetic protein signalling in airway epithelial cells during regeneration. *Cell. Signal.* 23, 398–406.
- McQualter, J.L., Yuen, K., Williams, B., and Bertoncello, I. (2010). Evidence of an epithelial stem/progenitor cell hierarchy in the adult mouse lung. *Proc. Natl. Acad. Sci. USA* 107, 1414–1419.
- Minami, T., Horiuchi, K., Miura, M., Abid, M.R., Takabe, W., Noguchi, N., Kohro, T., Ge, X., Aburatani, H., Hamakubo, T., et al. (2004). Vascular endothelial growth factor- and thrombin-induced termination factor, Down syndrome critical region-1, attenuates endothelial cell proliferation and angiogenesis. *J. Biol. Chem.* 279, 50537–50554.
- Morrison, S.J., and Spradling, A.C. (2008). Stem cells and niches: mechanisms that promote stem cell maintenance throughout life. *Cell* 132, 598–611.
- Mou, H., Zhao, R., Sherwood, R., Ahfeldt, T., Lapey, A., Wain, J., Sicilian, L., Izvolsky, K., Musunuru, K., Cowan, C., and Rajagopal, J. (2012). Generation of multipotent lung and airway progenitors from mouse ESCs and patient-specific cystic fibrosis iPSCs. *Cell Stem Cell* 10, 385–397.
- Nolan, D.J., Ginsberg, M., Israely, E., Palikuqi, B., Poulos, M.G., James, D., Ding, B.S., Schachterle, W., Liu, Y., Rosenwaks, Z., et al. (2013). Molecular signatures of tissue-specific microvascular endothelial cell heterogeneity in organ maintenance and regeneration. *Dev. Cell* 26, 204–219.
- O’Shea, K.S., and Dixit, V.M. (1988). Unique distribution of the extracellular matrix component thrombospondin in the developing mouse embryo. *J. Cell Biol.* 107, 2737–2748.
- Otto, W.R. (2002). Lung epithelial stem cells. *J. Pathol.* 197, 527–535.
- Rawlins, E.L., Okubo, T., Xue, Y., Brass, D.M., Auten, R.L., Hasegawa, H., Wang, F., and Hogan, B.L. (2009). The role of Scgb1a1+ Clara cells in the long-term maintenance and repair of lung airway, but not alveolar, epithelium. *Cell Stem Cell* 4, 525–534.
- Rock, J.R., Onaitis, M.W., Rawlins, E.L., Lu, Y., Clark, C.P., Xue, Y., Randell, S.H., and Hogan, B.L. (2009). Basal cells as stem cells of the mouse trachea and human airway epithelium. *Proc. Natl. Acad. Sci. USA* 106, 12771–12775.
- Rock, J.R., Barkauskas, C.E., Counce, M.J., Xue, Y., Harris, J.R., Liang, J., Noble, P.W., and Hogan, B.L. (2011). Multiple stromal populations contribute to pulmonary fibrosis without evidence for epithelial to mesenchymal transition. *Proc. Natl. Acad. Sci. USA* 108, E1475–E1483.
- Rosendahl, A., Pardali, E., Speletas, M., Ten Dijke, P., Heldin, C.H., and Sideras, P. (2002). Activation of bone morphogenetic protein/Smad signaling in bronchial epithelial cells during airway inflammation. *Am. J. Respir. Cell Mol. Biol.* 27, 160–169.
- Ryeom, S., Baek, K.H., Rieth, M.J., Lynch, R.C., Zaslavsky, A., Birsner, A., Yoon, S.S., and McKeon, F. (2008). Targeted deletion of the calcineurin inhibitor DSCR1 suppresses tumor growth. *Cancer Cell* 13, 420–431.
- Sountoulidis, A., Stavropoulos, A., Giaglis, S., Apostolou, E., Monteiro, R., Chuva de Sousa Lopes, S.M., Chen, H., Stripp, B.R., Mummery, C., Andreakos, E., and Sideras, P. (2012). Activation of the canonical bone morphogenetic protein (BMP) pathway during lung morphogenesis and adult lung tissue repair. *PLoS One* 7, e41460.
- Teisanu, R.M., Chen, H., Matsumoto, K., McQualter, J.L., Potts, E., Foster, W.M., Bertoncello, I., and Stripp, B.R. (2011). Functional analysis of two distinct bronchiolar progenitors during lung injury and repair. *Am. J. Respir. Cell Mol. Biol.* 44, 794–803.
- Tropea, K.A., Leder, E., Aslam, M., Lau, A.N., Raiser, D.M., Lee, J.H., Balasubramanian, V., Fredenburgh, L.E., Alex Mitsialis, S., Kourembanas, S., and Kim, C.F. (2012). Bronchioalveolar stem cells increase after mesenchymal stromal cell treatment in a mouse model of bronchopulmonary dysplasia. *Am. J. Physiol. Lung Cell. Mol. Physiol.* 302, L829–L837.
- Vintersten, K., Monetti, C., Gertsenstein, M., Zhang, P., Laszlo, L., Biechele, S., and Nagy, A. (2004). Mouse in red: red fluorescent protein expression in mouse ES cells, embryos, and adult animals. *Genesis* 40, 241–246.
- Wright, D.E., Cheshier, S.H., Wagers, A.J., Randall, T.D., Christensen, J.L., and Weissman, I.L. (2001). Cyclophosphamide/granulocyte colony-stimulating factor causes selective mobilization of bone marrow hematopoietic stem cells into the blood after M phase of the cell cycle. *Blood* 97, 2278–2285.
- Zacharek, S.J., Fillmore, C.M., Lau, A.N., Gludish, D.W., Chou, A., Ho, J.W., Zamponi, R., Gazit, R., Bock, C., Jäger, N., et al. (2011). Lung stem cell self-renewal relies on BMI1-dependent control of expression at imprinted loci. *Cell Stem Cell* 9, 272–281.